



ISSN: 2230-9926

Available online at <http://www.journalijdr.com>

IJDR

International Journal of Development Research

Vol. 11, Issue, 11, pp. 51670-51675, November, 2021

<https://doi.org/10.37118/ijdr.23301.11.2021>



RESEARCH ARTICLE

OPEN ACCESS

ANALYSIS OF THE M.A.C® HEALING ACCELERATION METHODOLOGY IN A MUSCLE INJURY

Marcus V. M. Pinto^{1,*}, Nilton P. Vilardi J.R.², Felipe Petrone³, Aline R. Sampaio⁴, Esteban Fortuny⁵, Thaís P. P. Passos⁶, Patricia F. Mayer⁷, Mariel P. Oliveira Junior⁸ and Miriam V. Baron⁹

¹PhD and creator of the MAC® Method. CEO and Researcher of the Celulare Institute, Petrópolis, Rio de Janeiro, Brazil; ²Physiotherapist. Researcher and Fluminense Football Club. Rio de Janeiro RJ, Brazil; ³Sp. Physiotherapist and researcher of the Celulare Institute. Petrópolis, Rio de Janeiro, Brazil; ⁴Physiotherapist and Researcher at Universidad Finis Terrae. CEO of Researcher and Diagnostra. Santiago, Chile; ⁵Physiotherapist of Macae City. Rio de Janeiro, Brazil; ⁶PhD in Health Sciences, Professor of the Physiotherapy course at the Rio Grande do Norte University Center, Brazil; ⁷Master Student in Health and Technology in the Hospital Space. Federal University of State of Rio de Janeiro (UNIRIO), Bezerra de Araújo College (FABA). Rio de Janeiro, Brazil; ⁸Medical student at the School of Medicine of the Pontifical Catholic University of Rio Grande do Sul (PUC/RS), Porto Alegre, Brazil

ARTICLE INFO

Article History:

Received 17th August, 2021
Received in revised form
28th September, 2021
Accepted 11th October, 2021
Published online 23rd November, 2021

Key Words:

M.A.C. Injury Sports.
Muscular Regeneration.

*Corresponding author:

Marcus P. M. Pinto

ABSTRACT

Overuse injuries are common in elite athletes. The repetitive forces of sports activities lead to tendon, muscle, cartilage, bone, and nerve injuries and poor physical performance. An accurate and early diagnosis is necessary to design an objective and assertive rehabilitation program so that the athlete can return to his or her professional activities as soon as possible. This is the objective of this case report that used in a professional athlete of the Fluminense Futebol Clube, the M.A.C. Method - cicatricial acceleration method for the recovery of a muscular injury grade 2 of the semi-tendineus, verified after ultrasonography exam and that was positive compared to the magnetic resonance imaging. The treatment started on 03/25/2021 with the MAC methodology and ended on 03/28/2021. On 03/29/2021 the athlete was released to return to his club activities with the team. The M.A.C. application was done once a day, combining methylene blue with cryotherapy, which was used before and after the methodology. The M.A.C. Methodology doping therapy was used with the athlete: Red Laser:1200s/900s/600s, Amber Led:1800s/1200s/900s. The results of the therapy with the M.A.C. were qualified by the pain VAS scale where on the first day of care VAS = 7, on the third day VAS = 2 and on the fourth day VAS = 1. And they were quantified using ultrasound imaging from the first day of injury to the final response of the athlete's treatment with the M.A.C. methodology. Hamstring Muscle Injuries are prevalent in many sports, including soccer, and are often associated with prolonged time away from sport due to the long recovery process that a classic rehabilitation program takes, and where the athlete can course to functional decline and risk of new injuries. The scientific literature suggests that rehabilitation programs should be improved after ischiotibial muscle injury because there is still no consensus on the best methodology for faster recovery and return of the athlete to his/her activities. The M.A.C. methodology proved to be effective as part of the rehabilitation program in the recovery of the semi-tendinous muscle injury in high performance athletes in a short period of time, favoring the return of the professional to the game and minimizing possible disability.

Copyright © 2021, Marcus P. M. Pinto et al. This is an open access article distributed under the Creative Commons Attribution License, which permits unrestricted use, distribution, and reproduction in any medium, provided the original work is properly cited.

Citation: Marcus P. M. Pinto, Nilton P. Vilardi J.R., Felipe Petrone, Aline R. Sampaio, Esteban Fortuny et al. "Analysis of the m.a.c® healing acceleration methodology in a muscle injury", *International Journal of Development Research*, 11, (11), 51670-51675.

INTRODUCTION

Muscle injuries of the hamstrings are very common in soccer practice and are the most common cause of functional disability in soccer athletes. It is estimated that 30 to 50% of all sports-related injuries worldwide are caused by soft tissue injuries (Herring & Nilson, 1987). Although the non-surgical treatment results in a good clinical and physiotherapeutic prognosis in most soccer athletes with grade II semi-tendinous muscle injury, the consequences of failed therapeutic treatment can be dramatic, delaying the return to sports activities for weeks or even months (Pedrinelli et al., 2006). The knowledge of some basic principles of tissue regeneration and the mechanisms of

functional repair of the affected muscle can collaborate clinically and avoid imminent pathognomonic dangers and accelerate the return to soccer.

Anatomy and biomechanics: The fibers of muscle tissue generally have their anatomical and functional origin in a fixed bony or tendinous elastic base. There are muscles that traverse one or more joints to generate movement. Muscles with tonic or postural function are usually uni-articular, wide, flat, with low contraction speed, and with a large capacity to generate and maintain contractile force. They are usually located in the deeper compartments. Bi-articular muscles have greater contraction speed and capacity for length change, but less ability to withstand tension. They are usually located in

superficial compartments. As to shape, the fusiform muscles allow a greater range of motion, while the pennate muscles have greater contractile strength. Fiber length is an important determinant of the amount of contraction possible in muscle. Because muscle fibers generally have an oblique distribution within a muscle belly, they are generally shorter than the overall length of the muscle.

Injury Mechanisms: Muscle injuries can be caused by contusions, strains, or tears. More than 90% of all sports-related injuries are contusions or strains (Järvinen & Lehto, 1993). Muscle lacerations, on the other hand, are the least frequent injuries in sports. The tensile force exerted on the muscle leads to excessive stretching of the myofibrils and, consequently, to a rupture near the myotendinous junction. Muscle stretches are typically seen in superficial muscles that work across two joints, such as the rectus femoris, semitendinosus, and gastrocnemius muscles.

Classification: Currently, the classification of muscle injuries separates injuries into mild, moderate, and severe based on clinical and functional aspects (Pedrinelli *et al.*, 2006). Characterized mild (grade I) strains and contusions represent injury to only a few muscle fibers with minor infiltrating edema and clinical discomfort on mild exertion, accompanied clinically by no or minimal loss of strength and restriction of functional movement. It is not feasible to palpate any muscle damage during maximal muscle contraction. Although the pain mechanism does not cause significant clinical disability, keeping the soccer athlete active is not recommended because of the high risk of increasing injury extensibility (Hernandez, 1996). Moderate (grade II) strains and contusions cause greater tissue damage to the muscle with evident loss of function. It is possible to palpate a small muscular injury, or clinical gap, at the actual injury site, with the formation of a discrete local hematoma with eventual ecchymosis sign within two to three days. The functional evolution for muscle healing usually takes two to three weeks and, after about a month, the patient can return to physical activity in soccer in a slow and gradual way (Hernandez, 1996). A hamstring muscle injury in soccer extends across the entire transverse section of the hamstring muscle and thus results in a complete loss of severity (grade III). The failure of muscle architecture is evident, and the ecchymosis is usually extensive, often distant from the site of muscle breakdown. The healing time for this injury ranges from four to six weeks. This type of hamstring injury requires classic, intense rehabilitation for long periods of up to three to four months. The patient may remain with some degree of pain and functional disability for months after the clinical occurrence and treatment of the injury (Hernandez, 1996).

Physiopathology

What distinguishes muscle injury healing from bone healing is that in muscle a repair process occurs, while in bone tissue a regeneration process occurs in the muscle fibers.

Muscle healing follows a constant order, without major changes depending on the causal element (contusion, stretch or tear).

Three clinical phases have been identified in this process: destruction, repair, and remodeling. The last two phases (repair and remodeling) overlap and are closely related.

Phase 1: Destruction - characterized by rupture and subsequent necrosis of the myofibrils, by the formation of intra-muscle hematoma in the space formed between the ruptured muscle and by the proliferation of inflammatory cells.

Phase 2: Repair and remodeling - consists of intense phagocytosis of necrotic tissue, regeneration of myofibrils, and concomitant production of connective scar tissue, as well as vascular neoformation and neural growth.

Phase 3: Remodeling - period of maturation of the regenerated myofibrils, of contraction and reorganization of the scar tissue and of recovery of the functional muscular capacity as a whole.

Because myofibrils are fusiform and very long, there is an imminent risk that necrosis initiated at the site of injury will extend along the entire length of the fiber. However, there is a specific structure, called the contraction band, which is a condensation of cytoskeletal material that acts as a "muscle system" (Hurme *et al.*, 1991). Once the destruction phase subsides, the present repair of muscle injury begins with two simultaneous and competing processes: the regeneration of the ruptured myofibril and the formation of scar connective tissue. A balanced progression of these processes is a prerequisite for optimal recovery of muscle contractile function (Hurme *et al.*, 1991). Although myofibrils are generically considered non-mitotic, the regenerative capacity of skeletal muscle is ensured by an intrinsic mechanism that restores the injured contractile apparatus. During embryonic development, a reserve pool of undifferentiated cells, called satellite cells, is stored below the basal lamina of each myofibril. In response to injury, these cells first proliferate, differentiate into myofibrils, and finally join together to form multinucleated myotubules (Rantanen *et al.*, 1995). Over time, the scar formed diminishes in size, leading the edges of the injury to adhere more closely to each other. However, it is not known whether the transection of the myofibrils on the opposite sides of the scar will definitely fuse together or whether a connective tissue septum will form between them (Aärimaa *et al.*, 2004). Immediately after muscle injury, the gap formed between the ruptured muscle fibers is filled with hematoma. Within the first day, inflammatory cells, including phagocytes, invade the hematoma and start to organize the clot (Cannon & St Pierre, 1998). Blood-derived fibrin and fibronectin intercalate to form granulation tissue, an initial framework and site anchoring for recruited fibroblasts (Hurme *et al.*, 1991). More importantly, this newly formed tissue provides the initial tensile property to resist the contractions applied against it. Approximately ten days after the trauma, the scar matures to a point where it is no longer the most fragile site of the muscle injury (Kääriäinen *et al.*, 1998). Although most skeletal muscle injuries heal without the formation of disabling fibrous scar tissue, fibroblast proliferation can be excessive, resulting in the formation of dense scar tissue within the muscle injury. A vital process for the regeneration of injured muscle is the area of vascularization. The restoration of the vascular supply is the first sign of regeneration and a prerequisite for subsequent morphological and functional recoveries and what we propose in this article (Järvinen, 1976).

CASE REPORT

Patient M.G.B., 34 years old, professional athlete of Fluminense Football Club, with complaint of pain in the posterior region of the right thigh, feeling the thigh "heavy and stuck". After ultrasound examination, a grade 2 semi-tendinous muscle injury was found, compared to an MRI scan that was positive for this injury. Treatment started on 03/25/2021 with the M.A.C methodology and ended on 03/28/2021. (Figure 1 and 2). The treatment consisted of applying the M.A.C methodology once a day, combined with methylene blue and cryotherapy before and after the use of the methodology. On 03/29/2021 the athlete was released to start his return to work practice.

An analog pain scale, VAS, was used

On the first day VAS = 7

On the third day VAS = 2

On the fourth day VAS = 1

The doping therapy of the M.A.C Methodology was used with the athlete:

Red Laser: 1200s/900s/600s

Amber Led: 1800s/1200s/900s

M.A.C. METHOD: Conventional methods of laser light emission (LLLT)/LED are based on biphasic response demonstrated many times in LLLT research and as with other forms of drugs, LLLT has its active ingredients or "drug" (irradiation parameters) and a "dose" (the irradiation time) and the "Arndt-Schulz Law" is often cited as a suitable model to describe the dose dependent effects of LLLT (Chung *et al.*, 2012; Huang *et al.* (2011).

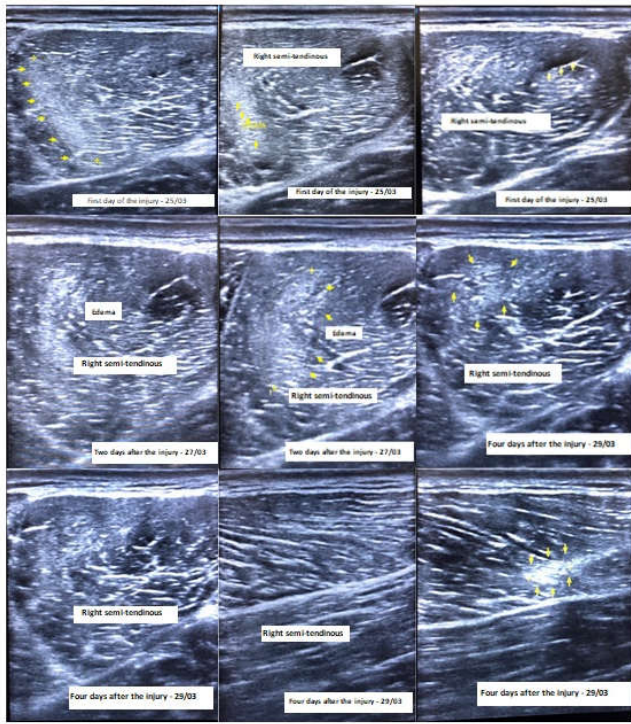


Figure 1. MRI Guided Ultrasound Images, proving the Injury Mechanism and the Therapeutic Response of the M.A.C. Methodology

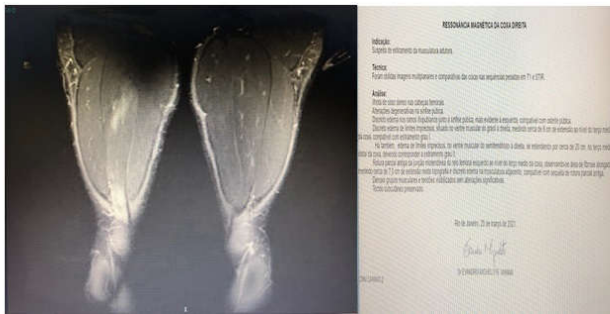
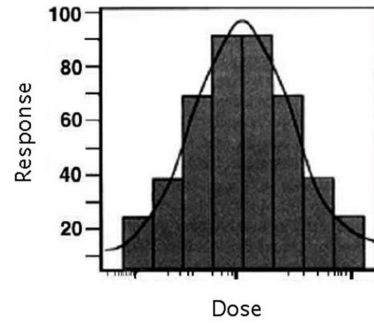


Figure 2. Nuclear Magnetic Resonance Imaging for Diagnosis

The concept of the Arndt-Schulz Law dates back to the years around the end of the 19th century, when H. Schulz published a series of papers examining the activity of various types of poisons (iodine, bromine, mercuric chloride, arsenic acid, etc.) on yeast, showing that almost all of these agents have a mildly stimulatory effect on yeast metabolism when administered in low doses. He then got in touch with the psychiatrist R. Arndt and together they developed a principle that later became known as the 'Arndt-Schulz law', stating that weak stimuli slightly accelerate vital activity, stronger stimuli increase it further, but a peak is reached and even stronger stimuli suppress it, until a negative response is finally reached (Huang *et al.*, 2011). Huang *et al.* (2011) reported the molecular effects at biphasic dose of LLLT, where low levels of light have a much better effect on tissue stimulation and repair than higher levels of light. A "biphasic" curve was used to illustrate the expected dose response to light at a subcellular, cellular, tissue or clinical level. Simply put, it suggests that if insufficient energy is applied, there will be no response (because the minimum threshold has not been reached), if more energy is applied, then a threshold is crossed and biostimulation is achieved, but when too much energy is applied, then the stimulation disappears and is replaced by bioinhibition (Figure 3). According to the authors, this 3D model shows a possible "sweet spot" of dose to the target tissue. This model suggests that insufficient power density or too short a time will have no effect on pathology, that too much power density and/or time may have inhibitory effects, and that there

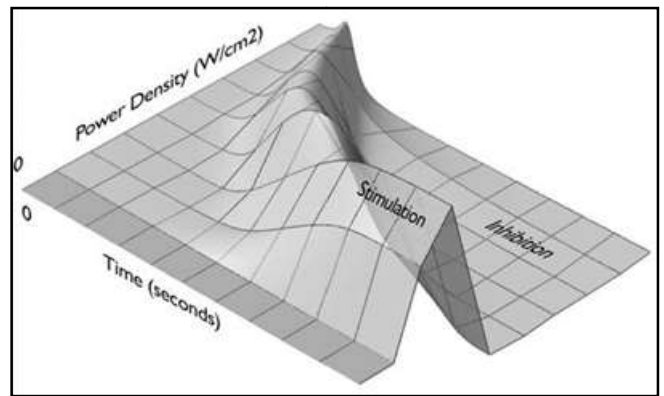
may be an optimal balance between power density and time that produces a maximum beneficial effect.



Source: Huang *et al.* (2011).

Figure 3. Biphasic curve illustrating dose response to light

In 2011, Huang *et al.* (2011), created a three-dimensional model of the Arndt-Schulz curve illustrating the thesis of how irradiance or illumination time (fluence) can have biphasic dose response effects in LLLT (Figure 4).

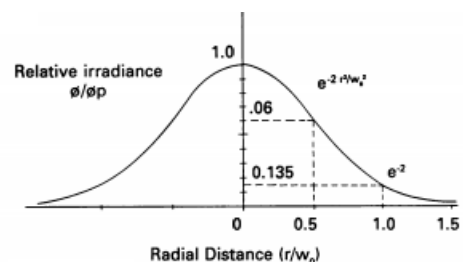


Source: Huang *et al.* (2011).

Figure 4 - 3D model of the Arndt-Schulz curve.

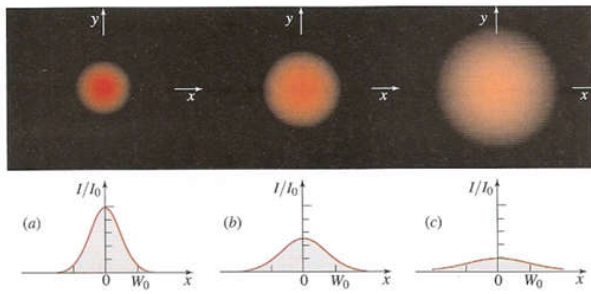
There may even be a (low) power density for which infinite irradiation time would have only positive effects and no inhibitory effects.

The M.A.C. Methodology: The method is based on clinical sovereignty with accurate diagnostic instruments for tissue assessment of open wounds and tissue injuries in need of repair (tegumentary tissue, striated skeletal muscle, bone and cartilage). The M.A.C. uses photodynamic therapy with the use of photopharmaceuticals, cellular markers and the use of correct parameters for each case inducing the acceleration of tissue repair. Photodynamic therapy (PDT) is a photochemical-based approach that uses light to activate specific chemicals that, in the activated state, confer cytotoxicity. It involves three main components: a photosensitizer, a light source, and tissue oxygen. When these components are combined, they become toxic to the target cells (Hernandez, 1996).



Source: Welch *et al.* (1989).

Figure 5. Gaussian Beam



(a) $z = 0$; (b) $z = z_0$; (c) $z = 2z_0$. Source: Saleh and Teich (2007).

Figure 6. Normalized beam intensity, I/I_0 , as a function of radial distance ρ at different axial distances

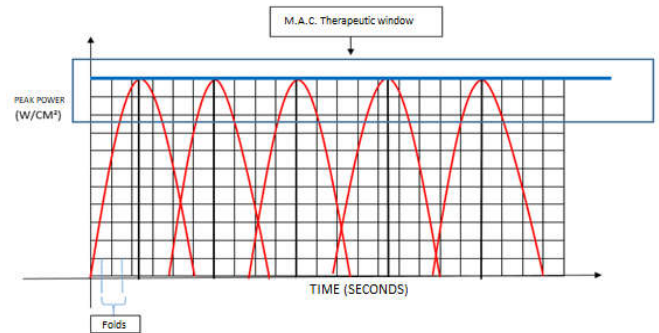
The correct light emission parameters need to be appropriate to excite the photosensitizer and produce reactive oxygen species " ROS " and accelerate ATP production (Hurme *et al.*, 1991). For this, M.A.C. uses doping in two treatment modalities as Monodoses and Doses. Therefore, it is necessary to evaluate the type of tissue, taking into consideration its density, redox states, severity and depth of the tissue injury, type of microorganism that may be colonizing the tissue. Another important factor is the qualitative measurement of the basal temperature of the skin, where tissues with higher temperature and/or irradiance require less dosimetry, and tissues with lower irradiance require higher dosimetry. Monodoses are subdoses. It is used time fold over time, fractioning the time in each wavelength. This doubling of time can be increasing or decreasing depending on the time of the comorbidities (chronic or acute), the characteristics of the injury, the objective of the treatment, the clinical evaluation. Dosimetry is increased or decreased depending on each case. Doses are fixed time folds at each wavelength. The dose is medialized. It is most often used in organisms where metabolism is high upon clinical evaluation. Example athletes, children.

Laser Physics X M.A.C: Spatio-temporal control over the intensity of a laser/LED pulse has the potential to enable or revolutionize a wide range of laser-based applications. Currently, laser applications suffer from little flexibility by conventional optics that provide little or no control over the trajectory of the peak intensity (Simpson *et al.*, 2020). Conventional optics relies only on spatial formation, for example by refraction or diffraction, which severely restricts its flexibility (Simpson *et al.*, 2020). Most of the time, the laser beam assumes a Gaussian shape (from a normal distribution). This makes it more difficult to determine the exact irradiance (W/cm^2) at any point in the beam. There is peak irradiance, and the irradiance decreases with distance from the center of the beam. As the power is increased, the irradiance at the tail of the Gaussian profile increases and the distance of the critical limit from the beam center becomes larger (Figure 5 and 6). At any value of z , the intensity of the Gaussian beam is a function of the radial distance ρ . The Gaussian function has its largest value on the z -axis, with $\rho = 0$, and slowly decreases with increasing ρ . The width $W(z)$ of a Gaussian distribution increases with axial distance z . In more recent spatio-temporal pulse modeling schemes, called "self-flying focus" techniques, can produce symmetric cylindrical intensity peaks that propagate at any velocity over distances much greater than a Rayleigh band. When temporal pulse modeling is combined with the self-flying focus model, the collapse point can move at an arbitrary constant velocity through the collapse region.

$$\frac{P(t)}{P_c} = \left[\left(\frac{w_i}{w_f} \right) \left(\frac{1}{z_c(t)/f} - 1 \right) \right]^2 + 1,$$

The above equation expresses the laser power in the ratio of $P(t)/P(c)$, where w_f is a linear focal point. The t represents time with the pulse. And this is different when the time slice collapses. That is, by performing the integration of $z_c(t)$ and rearranging the terms, we raise the equation to another dimension, and this provides a reduction in the speed of the peak power. The M.A.C. Method resembles the technique for spatio-temporal control; the "self-flying focus"

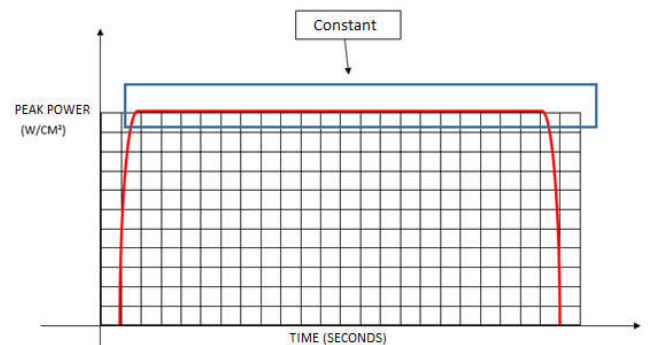
produces an arbitrary trajectory intensity peak that can be sustained for distances comparable to the focal length. The technique combines temporal pulse modeling and the inherent nonlinearity of a medium to customize the time and place at which each temporal slice within the pulse reaches its focus. With the doubling of time over time the parabolic profile of the wave amplitude begins to change tending to maintain and control the velocity of the laser/LED peak irradiance, controlling the divergence of the beam over a long distance, increasing and concentrating power and the therapeutic window without declining (Figures 7 and 8).



Source: Elaborated by the author (2021).

Figure 8. Graphic scheme of the folds in space - time keeping control of the peak laser/LED power velocity keeping a constant therapeutic window

When we use light therapy based on the M.A.C. method, it is necessary to evaluate the light-emitting system, the property of the electric field of matter through which this light propagates to evaluate the time of the folds in space-time and to aim the therapeutic result. It is known about the difference between the laser and the LED, where the former emits a coherent and collimated light and the latter a non-collimated and non-coherent light. In a collimated light emission, the energy deposited in the tissue is greater, requiring less energy density and in a non-collimated light emission (LED) the deposited energy is lower, requiring more time in the space-time folds, but the LED therapy covers larger body areas. Lambert-Beer's law (also called Lambert-Beer-Bouguer law) provides an accurate description of the effects arising from the interaction between light and matter. It establishes a relationship between the absorbance of a solution and its concentration when passed through a collimated monochromatic light radiation (parallel light rays). But, there are deviations from the Lambert - Beer law in the scientific literature.



Source: Elaborated by the author (2021).

Figure 8. Graphic scheme of the folds in space - time keeping control of the peak laser/LED power velocity keeping a constant therapeutic window

According to Mayerhöfer *et al.* (2020), electromagnetic theory defines that it is not the absorption rate, which is proportional to the concentration, but the imaginary part of the average polarizability. Molecules and ions present in the tissue are able to absorb photons and are then promoted from the fundamental state to a more energetic

excited state (Mayerhöfer *et al.*, 2020). Most molecules or unit cells are anisotropic, i.e. the characteristic that their physical properties vary with direction which justifies the biological effect on tissue by uncollimated light. The wavelength at which a certain substance will absorb light radiation is characteristic of its structure, and differs from substance to substance. Inhomogeneities can strongly alter absorbance spectra, in particular for biological samples consisting of tissue or cells (Mayerhöfer *et al.*, 2020).

Biophysical Modeling for M.A.C. Methodology: Nowadays mathematical modeling can provide independent insight into a biological process, and it is possible to generate theoretical predictions that could not have been predicted in advance, so mathematical models should form a crucial part of research in any biological process, including the M.A.C. Methodology.

This methodology aims at therapeutic applications of bio-stimulation (bio-modulation), from here we developed a time curve modeling for the M.A.C. Methodology

Main parameters for continuous dose applications

Note: The units in brackets represent the symbol of the physical quantities used in the calculations.

Dose [J] = D

Equivalent Dose Density (Fluence) [J/cm²] = Dose [J]/ Irradiated Area [cm²]

Laser Power [W] = P

Dose Application Time (s) = T (over the irradiated area)

Area at beam exit [cm²] = S₀

Numerical beam aperture = N.A.

Distance from the beam exit to the irradiated surface [cm] = h

Irradiated Area [cm²] = S

Power density = P/S [W/Cm²]

Number of Irradiated Areas = N

Irradiated Area Formula S

$$S \approx S_0 + \pi \cdot h^2 \cdot (N.A)^2$$

Formula of Dose D irradiated in an Area S

$$D = (P \times \Delta t)$$

Formula for the calculation of the Dose D irradiated in N areas S

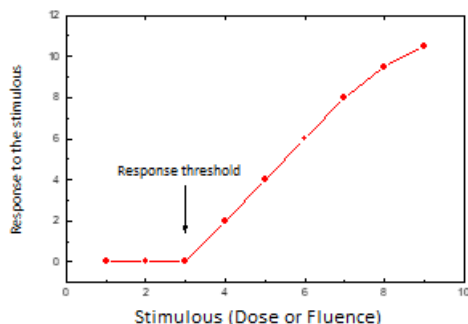
$$D = (P \times \Delta t)$$

Formula for calculating Equivalent Dose Density (Fluence) F_e in one area S

$$F_e [J/cm^2] = \text{Dose [J]} / \text{Irradiated Area [cm}^2\text{]}$$

$$F_e = (P \times \Delta t) / S$$

Note: The concept of Equivalent Dose Density (fluence) has the scientific rigor required for applications in stimulated processes that have thresholds as illustrated in the graph below (Figure 9).



Example 01

Figure 9. Example of Application (fixation) of the Concepts

Consider the following example to fix the concepts: A healthcare professional applies the following stimulus to a biological surface:

100 mW of continuous power at a wavelength of 660 nm (red) for 20 seconds on four different regions of the surface to be treated therapeutically. The four areas were irradiated with the nozzle of the equipment in contact with the surface.

DATA:

Number of Irradiated Areas N = 4

Nozzle area S₀ = 0.018 cm² (1.5 mm optical diameter)

Distance from the beam exit to the irradiated surface h = 0 (Eq. 1, nozzle in contact S = S₀)

Calculation of the Irradiated Dose in each region of the irradiated surface (Eq. 2)

$$D = 100 \times 10^{-3} \text{ W} \times 20 \text{ s} = 2000 \times 10^{-3} \text{ J} = 2.0 \text{ J}$$

Calculation of the total irradiated dose (Eq. 3):

$$D_N = 4 \times D = 8.0 \text{ J}$$

Calculation of Equivalent Dose Density (Fluence) F_e in each area S:

$$F_e [J/cm^2] = \text{Dose [J]} / \text{Irradiated Areas [cm}^2\text{]} = 2.0 \text{ J} / 0.018 \text{ cm}^2$$

$$F_e = 111 \text{ J/cm}^2$$

Calculation of Total Equivalent Dose Density (Total Fluence F_{eT}) applied to the surface:

$$F_{eT} = N \times F_e = 4 \times 111 \text{ J/cm}^2 = 444 \text{ J/cm}^2$$

Equivalent Power Density Calculation;

$$P/S = 100/0.018 \text{ mW/Cm}^2$$

$$P/S = 5.6 \text{ W/Cm}^2$$

Example 02

Consider the following example to fix the concepts: A healthcare professional applies the following stimulus to a biological surface:

120 mW of continuous power at a wavelength of 790 nm (infrared) for 20 seconds on a single region of the surface to be treated therapeutically. The area was irradiated with the nozzle of the equipment at a distance of 1 cm from the surface. The numerical aperture of the nozzle e' N.A. = 0.4

DATA:

Number of Irradiated Areas N = 1

Numerical Opening N.A = 0.4

Nozzle area S₀ = 0.018 cm² (1.5 mm optical diameter)

Distance from the beam exit to the irradiated surface h = 1 cm (Eq. 1, non-contact nozzle)

Irradiated area (Eq 1) S = 0.018 + 0.503 = 0.52 cm²

Calculation of the Irradiated Dose in each region of the irradiated surface (Eq. 2)

$$D = 120 \times 10^{-3} \text{ W} \times 20 \text{ s} = 2400 \times 10^{-3} \text{ J} = 2.4 \text{ J}$$

Calculation of the total irradiated dose (Eq. 3):

$$D_N = 1 \times D = 2.4 \text{ J}$$

Calculation of Equivalent Dose Density (Fluence) F_e in each area S:

$$F_e [J/cm^2] = \text{Dose [J]} / \text{Irradiated Area [cm}^2\text{]} = 2.4 \text{ J} / 0.52 \text{ cm}^2$$

$$F_e = 4.6 \text{ J/cm}^2$$

Equivalent Power Density Calculation;

P/S = 120/0.52 mW/Cm²
 P/S = 0.23 W/Cm²

Final Considerations: In cellular respiration, more specifically in the mitochondrial crests, the folds in space/time made by the M.A.C. methodology accelerate electron transport consequently speeding up the process of reactive oxygen species (ROS) production, if more singlet oxygen is produced (¹O₂) which is a very excitable oxygen, primordial for triggering biochemical actions and increased ATP production. This is due to the fact that the method uses unconventional optics in the use of lasers and LEDs. When the photon emission time is doubled, the cell responds because the stimulus is maintained without changing the peak power density velocity, without decline or bio-inhibition. The M.A.C. methodology demonstrated to be effective as part of the rehabilitation program in the recovery from grade 2 semitendinous muscle injury in a high performance soccer athlete in a short period of time, favoring the return of the professional to sports activities, minimizing possible disability and answering the questioning of the scientific literature that suggests that the classic rehabilitation programs after injury of the ischiotibial muscle ("Hamstring Muscle Injury") should be reviewed due to the lack of consensus on which is the best methodology for faster recovery and return of the athlete to his activities.

ACKNOWLEDGMENTS

This study was funded in part by the Coordination of Improvement of Higher Level Personnel - Brazil (CAPES) - Finance Code 001. - Thanks to the Brazilian company Ecco Fibras in the person of Mr. Henrique Trajano for the scientific support of this article.

Conflicts of Interest: The authors declare having no conflict of interest regarding this article.

REFERENCES

- Aärimala, V., Kääriäinen, M., Vaittinen, S., Tanner, J., Järvinen, T., Best, T., & Kalimo, H. 2004. Restoration of myofiber continuity after transection injury in the rat soleus. *Neuromuscular Disorders*, 14(7), 421-428. doi: 10.1016/j.nmd.2004.03.009
- Cannon, J. G., & St Pierre, B. A. 1998. Cytokines in exertion-induced skeletal muscle injury. *Molecular and Cellular Biochemistry*, 179(1-2), 159-167. doi: 10.1023/a: 10068 28425418
- Chung, H., Dai, T., Sharma, S. K., Huang, Y. Y., Carroll, J. D., & Hamblin, M. R. 2012. The nuts and bolts of low-level laser (light) therapy. *Annals of Biomedical Engineering*, 40(2), 516-533. doi: 10.1007/s10439-011-0454-7
- Hernandez, A. J. 1996. Distensões e rupturas musculares. In: Camanho, G. L. *Patologia do joelho*. São Paulo: Sarvier. p. 132-138.
- Herring, S. A., & Nilson, K. L. 1987. Introduction to overuse injuries. *Clinics in Sports Medicine*, 6(2), 225-239. <https://pubmed.ncbi.nlm.nih.gov/3319201/>
- Huang, Y. Y., Sharma, S. K., Carroll, J., & Hamblin, M. R. 2011. Biphasic dose response in low level light therapy - an update. *Dose-Response*, 9(4), 602-618. doi: 10.2203/dose-response.11-009.hamblin
- Hurme, T., Kalimo, H., Lehto, M., & Järvinen, M. 1991. Healing of skeletal muscle injury: an ultrastructural and immunohistochemical study. *Medicine and Science in Sports and Exercise*, 23(7), 801-810. <https://pubmed.ncbi.nlm.nih.gov/1921672/>
- Järvinen, M. 1976. Healing of a crush injury in rat striated muscle. 3. A micro-angiographical study of the effect of early mobilization and immobilization on capillary ingrowth. *Acta Pathologica et Microbiologica Scandinavica. Section A, Pathology*, 84(1), 85-94. <https://pubmed.ncbi.nlm.nih.gov/1251736/>
- Järvinen, M. J., & Lehto, M. U. 1993. The effects of early mobilisation and immobilisation on the healing process following muscle injuries. *Sports Medicine (Auckland, N.Z.)*, 15(2), 78-89. doi: 10.2165/00007256-199315020-00002
- Kääriäinen, M., Kääriäinen, J., Järvinen, T. L., Sievänen, H., Kalimo, H., & Järvinen, M. 1998. Correlation between biomechanical and structural changes during the regeneration of skeletal muscle after laceration injury. *Journal of Orthopaedic Research*, 16(2), 197-206. doi: 10.1002/jor.1100160207
- Mayerhöfer, T. G., Pahlow, S., & Popp, J. 2020. The Bouguer-Beer-Lambert Law: shining light on the obscure. *Chemphyschem*, 21(18), 2029-2046. doi: 10.1002/cphc.202000464
- Pedrinelli, A., Fernandes, T. L., Thiele, E., & Teixeira, W. J. 2006. *Lesão muscular: ciências básicas, fisiopatologia, diagnóstico e tratamento*. In: Alves Júnior, W. M., Fernandes, T. D. *Programa de atualização em traumatologia e ortopedia (PROATO)*. Porto Alegre: Artmed. p. 10-32.
- Rantanen, J., Hurme, T., Lukka, R., Heino, J., & Kalimo, H. 1995. Satellite cell proliferation and the expression of myogenin and desmin in regenerating skeletal muscle: evidence for two different populations of satellite cells. *Laboratory Investigation*, 72(3), 341-347. <https://pubmed.ncbi.nlm.nih.gov/7898053/>
- Saleh, B. E. A., & Teich, M. C. 2007. *Fundamentals Of Photonics* (2a ed.). New Jersey: John Wiley & Sons.
- Simpson, T. T., Ramsey, D., Franke, P., Vafaei-Najafabadi, N., Turnbull, D., Froula, D. H., & Palastro, J. P. 2020. Nonlinear spatiotemporal control of laser intensity. *Optics Express*, 28(26), 38516-38526. doi: 10.1364/OE.4111011
- Vogt, S., Ansah, P., & Imhoff, A. B. 2007. Complete osseous avulsion of the adductor longus muscle: acute repair with three fiberwire suture anchors. *Archives of Orthopaedic and Trauma Surgery*, 127(8), 613-615. doi: 10.1007/s00402-007-0328-5
- Welch, A. J., Torres, J. H., & Cheong, W. F. 1989. Laser physics and laser-tissue interaction. *Texas Heart Institute Journal*, 16(3), 141-149. <https://pubmed.ncbi.nlm.nih.gov/15227198/>
